IEICE TRANS. FUNDAMENTALS, VOL. E79–A, NO. 9 SEPTEMBER 1996

PAPER

Analysis of Nonuniform and Nonlinear Transmission Lines via Frequency-Domain Technique

Yuichi TANJI†, *Student Member*, Yoshifumi NISHIO†, *and* Akio USHIDA†, *Members*

SUMMARY There are many kinds of transmission lines such as uniform, nonuniform and nonlinear ones terminated by linear and/or nonlinear subnetworks. The *nonuniform transmission lines* are crucial in integrated circuits and printed circuit boards, because these circuits have complex geometries and layout between the multi layers, and most of the transmission lines possess nonuniform characteristics. On the other hand, the *nonlinear transmission line* have been focused in the fields of communication and instrumentation. Here, we present a new numerical method for analyzing nonuniform and nonlinear transmission lines with linear and/or nonlinear terminations. The waveforms at any points along the lines are described by the Fourier expansions. The partial differential equations representing the circuit are transformed into a set of ordinary differential equations at each frequency component, where for nonlinear transmission line, the *perturbation technique* is applied. The method is efficiently applied to weakly nonlinear transmission line. The nonuniform transmission lines terminated by a nonlinear subnetwork are analyzed by *hybrid frequency-domain method.* The stability for stiff circuit is improved by introducing *compensation element.* The efficiency of our method is illustrated by some examples.

key words: *nonuniform transmission lines, nonlinear transmission line, perturbation technique, hybrid frequency-domain method, compensation element*

1. Introduction

The high-speed performance of microwave or digital circuit systems is limited by the interconnect effects rather than the switching speed of semiconductor devices. For high frequency signal, the dispersive of transmission lines is remarkable, and the delay, reflection phenomena and crosstalk cause many distortions of the transmitting waveform. Generally, these circuits are fabricated on a integrated circuit. To achieve the high density, complex geometries and layout between the multi layers are necessary. In this case, the transmission lines are considered as having nonuniform characteristics. Therefore, the analysis of nonuniform transmission lines is important for designing the high performance systems on VLSI circuits, printed circuit boards and multi-chip modules.

Recently, many papers about the transient analysis of nonuniform transmission lines have been published [1]–[5], where the nonuniformity is assumed by a piecewise stepping function. When the transmission lines have complicated structures, applying these methods is difficult due to the expensive computational cost. Palusinski and Lee [6] have proposed a spectral method with Chebyshev polynomials which can be applied to any kinds of nonuniform transmission lines. Dhaene, Martens and Zutter [7] have presented an efficient time-domain method based on the convolution technique to the scattering parameters. The method can be applied to any circuits whenever the parameters are derived by any techniques. Manney, Nakhla and Zhang [8] have applied the NILT (Numerical Inversion of Laplace Transform) to the transient analysis of nonuniform transmission lines, where they first get the solution in complex s domain, and NILT is used to get the time-domain response.

In this paper, we focus the steady-state analysis of nonuniform transmission lines with nonlinear termination is also important on the design of the microwave systems. Since transmission lines are equivalently described by the infinite number of state equations, we can not directly apply the time-domain shooting method [9] based on the transient analysis. Here, a partitioning technique in the time- and frequency-domain is presented, where a given circuit is partitioned into linear and nonlinear subnetworks. If the voltage and current waveforms of one subnetwork are exactly equal to the other at the partitioning point, it will give rise to the steady-state waveforms. The response for the linear subnetworks containing the nonuniform transmission lines can be calculated in the frequency-domain. If the response of nonlinear lumped subnetwork calculated in the time-domain is described in the frequency-domain, then, we can easily calculate the steady-state response [16]. For the nonuniform transmission lines, we do not place any restriction on the nonuniformity, but also assume frequency-dependent parameters. It is very important, because skin and proximity effects [10] are serious problems to high-speed VLSI circuits.

On the other hand, nonlinear transmission line is significant in the fields of communication and instrumentation. Especially, GaAs nonlinear transmission line is used for picosecond pulse compressions, broadband phase modulations [11] and picosecond shock-wave generations [12]. Nonlinear transmission line is described by nonlinear partial differential equation. Freeman and Karbowiak [13] have introduced the *difference approximation technique.* The draw back of this

Manuscript received November 16, 1995.

†The authors are with the Faculty of Engineering, Tokushima University, Tokushima-shi, 770 Japan.

method is great computational time, because we must finely discretize the time and spatial coordinates to get the accurate solution. Here, we propose a frequency-domain perturbation method such that nonlinear terms at each iteration are replaced by using the previous results [14]. In this case, the nonlinear partial differential equation is solved in a set of linear ordinary differential equations at each iteration. Our method can be efficiently applied to weakly nonlinear transmission line.

In Sects. 2 and 3, we propose a numerical method for analyzing the nonuniform transmission lines terminated by the nonlinear lumped subnetwork. In Sect. 4, we present a frequency-domain perturbation technique to analyze nonlinear transmission line. In Sect. 5, we show some illustrative examples.

2. Nonuniform Transmission Lines

Consider N-conductors transmission lines terminated by linear subnetworks as shown in Fig. 1, where the parameters per unit length are given by $\mathbf{R}(x,\omega)$, $\mathbf{L}(x,\omega)$, $\mathbf{C}(x,\omega)$ and $\mathbf{G}(x,\omega)$ which have nonuniform and frequency-dependent characteristics and they are functions of a distance x from near-end and a frequency ω containing in the transmitted signals.

Let the transmission lines be driven by pulse inputs of the period T. We describe the pulse inputs $\mathbf{e}(t)$ by the complex Fourier expansions as follows:

$$\mathbf{e}(t) = \sum_{k=-M}^{M} \mathbf{E}_k \exp(jk\omega_0 t) \tag{1}$$

for $\omega_0 = 2\pi/T$.

The circuit equations of the transmission lines are described by the following partial differential equations.

$$-\frac{\partial \mathbf{v}(x,t)}{\partial x} = \mathbf{R}(x,\omega)\ \mathbf{i}(x,t) + \mathbf{L}(x,\omega)\ \frac{\partial \mathbf{i}(x,t)}{\partial t} \tag{2.a}$$

$$-\frac{\partial \mathbf{i}(x,t)}{\partial x} = \mathbf{G}(x,\omega)\ \mathbf{v}(x,t) + \mathbf{C}(x,\omega)\ \frac{\partial \mathbf{v}(x,t)}{\partial t} \tag{2.b}$$

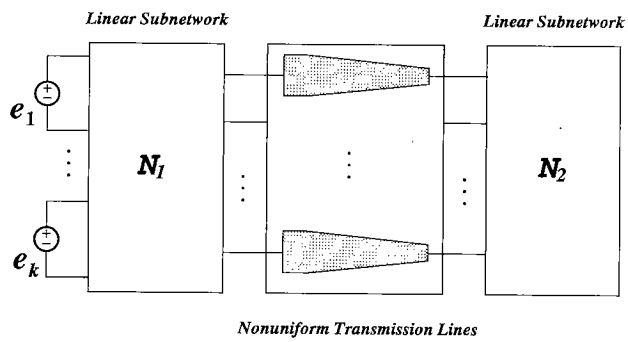

Fig. 1 N-conductors nonuniform transmission lines terminated by linear subnetworks.

We also assume the waveforms in the Fourier expansions as follows:

$$\mathbf{v}(x,t) = \sum_{k=-M}^{M} \mathbf{V}_k(x) \exp(jk\omega_0 t) \tag{3.a}$$

$$\mathbf{i}(x,t) = \sum_{k=-M}^{M} \mathbf{I}_k(x) \exp(jk\omega_0 t). \tag{3.b}$$

Substituing (3.a), (3.b) into (2.a), (2.b), they are transformed into the ordinary differential equations at each frequency component,

$$\frac{d}{dx}\begin{bmatrix} \mathbf{V}_k(x) \\ \mathbf{I}_k(x) \end{bmatrix} = \begin{bmatrix} \mathbf{0} & -\mathbf{Z}_k \\ -\mathbf{Y}_k & \mathbf{0} \end{bmatrix}\begin{bmatrix} \mathbf{V}_k(x) \\ \mathbf{I}_k(x) \end{bmatrix} \tag{4}$$

where

$$\mathbf{Z}_k = \mathbf{R}(x, k\omega_0) + jk\omega_0 \mathbf{L}(x, k\omega_0)$$
$$\mathbf{Y}_k = \mathbf{G}(x, k\omega_0) + jk\omega_0 \mathbf{C}(x, k\omega_0)$$

Put the solutions of (4)

$$\begin{bmatrix} \mathbf{V}_k(x) \\ \mathbf{I}_k(x) \end{bmatrix} = \mathbf{\Phi}_k(x)\begin{bmatrix} \mathbf{V}_k(0) \\ \mathbf{I}_k(0) \end{bmatrix} \tag{5}$$

where $\mathbf{\Phi}_k(x)$ is the fundamental matrix solution for k-th frequency component. Observe that the coefficient matrix of (4) depends on the geometrical structure of nonuniform transmission lines and it can be only solved numerically except for the special linear case.

Now, let us apply the boundary conditions to (5). At the input terminals, we have from the Thevenin's equivalent circuit theorem,

$$\mathbf{E}_{in,k} - \mathbf{Z}_{in,k}\ \mathbf{I}_k(0) = \mathbf{V}_k(0). \tag{6}$$

On the other hand, we assume at the output terminal:

$$\mathbf{V}_k(l) = \mathbf{Z}_{out,k}\ \mathbf{I}_k(l) \tag{7}$$

where $\mathbf{E}_{in,k}$ denotes the input voltage sources at kth frequency component, and l is the transmission line length. Combining (5), (6) and (7), we can get the responses at the both end points in the frequency-domain,

$$\begin{bmatrix} \mathbf{V}_k(0) \\ \mathbf{V}_k(l) \end{bmatrix} = -\left[\mathbf{A}_k + \mathbf{B}_k\mathbf{Y}_{1,k}\right]^{-1}\mathbf{B}_k\mathbf{Y}_{2,k}\begin{bmatrix} \mathbf{E}_{k,in} \\ \mathbf{0} \end{bmatrix} \tag{8}$$

where

$$\mathbf{A}_k = \begin{bmatrix} \mathbf{\Phi}_{k,11}(l) & -\mathbf{U} \\ \mathbf{\Phi}_{k,21}(l) & \mathbf{0} \end{bmatrix}$$

$$\mathbf{B}_k = \begin{bmatrix} \mathbf{\Phi}_{k,12}(l) & \mathbf{0} \\ \mathbf{\Phi}_{k,22}(l) & -\mathbf{U} \end{bmatrix} \tag{9.a}$$

$$\mathbf{Y}_{1,k} = \begin{bmatrix} -\mathbf{Z}_{in,k}^{-1} & \mathbf{0} \\ \mathbf{0} & \mathbf{Z}_{out,k}^{-1} \end{bmatrix}$$

$$\mathbf{Y}_{2,k} = \begin{bmatrix} \mathbf{Z}_{in,k}^{-1} & \mathbf{0} \\ \mathbf{0} & \mathbf{0} \end{bmatrix} \tag{9.b}$$

Thus, we can calculate the time-domain responses from (3.a), (8) and (9).

3. Hybrid Frequency-Domain Method

Now, we consider the nonuniform transmission lines terminated by a nonlinear subnetwork as shown in Fig. 2 (a), where N_i is a linear subnetwork which contains the transmission lines and N_n is a nonlinear subnetwork.

Using substitution theorem [17], the circuit can be partitioned into two subnetworks as shown in Fig. 2 (b). Then, we assume the substitution voltage sources $\mathbf{v}(t)$ as follows:

$$\mathbf{v}(t) = \sum_{k=-M}^{M} \mathbf{V}_k \exp(jk\omega_0 t). \tag{10}$$

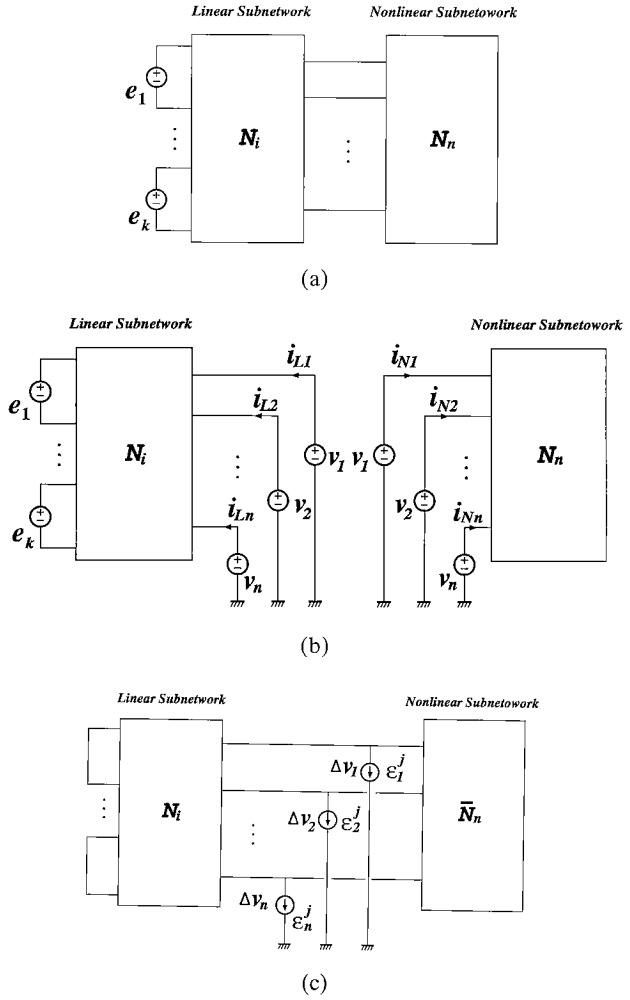

Fig. 2 (a) Nonuniform transmission lines terminated by a nonlinear subnetworks. (b) Partition the circuit into the linear and nonlinear subnetworks using substitution voltage sources $v_1(t), \ldots, v_n(t)$. (c) Sensitivity circuit for determining the variational values $\Delta v_1(t), \ldots, \Delta v_n(t)$.

The response of the linear subnetwork at the partitioning point can be calculated by (5), (6) and (10) as follows:

$$\mathbf{I}_{L,k} = \mathbf{H}_{k,21}\mathbf{E}_{in,k} + \mathbf{H}_{k,22}\mathbf{V}_k \tag{11}$$

where

$$\mathbf{H}_k = -[\mathbf{A}_k\mathbf{Z}_k - \mathbf{B}_k]^{-1}\mathbf{B}_k$$
$$\mathbf{Z}_k = \begin{bmatrix} \mathbf{Z}_{in,k} & \mathbf{0} \\ \mathbf{0} & \mathbf{0} \end{bmatrix}.$$

Using superposition theorem, the time-domain responses of the linear subnetwork $\mathbf{i}_L(t)$ are described by the Fourier expansions:

$$\mathbf{i}_L(t) = \sum_{k=-M}^{M} \mathbf{I}_{L,k} \exp(jk\omega_0 t). \tag{12}$$

On the other hand, the time-domain responses of the nonlinear subnetwork $\mathbf{i}_N(t)$ to the substitution voltage sources (10) are calculated by a numerical integration technique such as *backward difference formula* [18]. Then, we describe the responses $\mathbf{i}_N(t)$ by the Fourier expansions:

$$\mathbf{i}_N(t) = \sum_{k=-M}^{M} \mathbf{I}_{N,k} \exp(jk\omega_0 t). \tag{13}$$

The substitution theorem [17] says that if the substitution voltage sources $\mathbf{v}(t)$ satisfy

$$\mathbf{F}(\mathbf{v}(t)) \equiv \mathbf{i}_L(t) + \mathbf{i}_N(t) = \mathbf{0} \tag{14}$$

$\mathbf{v}(t)$ will be the output voltages at the far-end of transmission lines. Then, let us calculate the steady-state solutions satisfying (14) with an iterational method.

Assume the solutions at the $j+1$-st iteration,

$$\mathbf{v}^{j+1}(t) = \mathbf{v}^j(t) + \Delta\mathbf{v}(t) \tag{15}$$

where $\Delta\mathbf{v}(t)$ is the variational voltage waveforms described by

$$\Delta\mathbf{v}(t) = \sum_{k=-M}^{M} \Delta\mathbf{V}_k \exp(jk\omega_0 t). \tag{16}$$

Substituting $\mathbf{v}^{j+1}(t)$ from (15) into (14), we obtain

$$F(\mathbf{v}^j(t) + \Delta\mathbf{v}(t)) \equiv \mathbf{i}_L^{j+1}(t) + \mathbf{i}_N^{j+1}(t)$$
$$\simeq y_L^j(\Delta\mathbf{v}(t)) + y_{N,t}^j(\Delta\mathbf{v}(t)) + \varepsilon^j(t) = \mathbf{0}. \tag{17}$$

It is not easy to solve the time-varying circuit given by (17) even if it is a linear. Therefore, we introduce the following approximate equations:

$$y_L^j(\Delta\mathbf{v}(t)) + y_{N,0}^j(\Delta\mathbf{v}(t)) + \varepsilon^j(t) = \mathbf{0} \tag{18}$$

where the *residual errors* $\varepsilon^j(t)$ are defined by

$$\varepsilon^j(t) \equiv \mathbf{i}_L^j(t) + \mathbf{i}_N^j(t). \tag{19}$$

The symbols $\mathcal{Y}_L^j(\Delta\mathbf{v}(t))$, $\mathcal{Y}_{N,t}^j(\Delta\mathbf{v}(t))$ and $\mathcal{Y}_{N,0}^j(\Delta\mathbf{v}(t))$ in (17) and (18) denote *linear operators* which transform $\Delta\mathbf{v}(t)$ into the time-domain responses of the associated sensitivity subnetwork, where the subscript "t" denotes the time-varying operator and "0" the time-invariant operator, respectively [15].

Now, consider the equivalent circuit for determining $\Delta\mathbf{v}(t)$ satisfying (18). It has the same circuit configuration as the original one, except that the voltage sources are short-circuited and all of the nonlinear elements are replaced by time-invariant elements. At the partitioning point, it has current sources equal to the residual errors $\varepsilon^j(t)$ given by (19). Thus, we have the equivalent circuit as shown in Fig. 2 (c) and the Fourier coefficients of the variational voltages $\Delta\mathbf{V}_k$ at k-th frequency component can be easily obtained by the application of *phasor technique* to this circuit.

The iteration is continued until the variations satisfy

$$\| \Delta\mathbf{V} \| < \kappa \tag{20}$$

for a given small κ, where

$$\Delta\mathbf{V} = [\Delta V_0, \Delta V_1, \ldots, \Delta V_M]^T. \tag{21}$$

The residual errors after the iteration having converged are given by [9]

$$\delta^j = \frac{1}{T}\int_0^T [\| \mathbf{i}_L^j(t) + \mathbf{i}_N^j(t) \|]^2 dt = \sum_{k=2M+1}^{\infty} \| \mathbf{I}_{N,k}^j \|^2 . \tag{22}$$

If the residual errors are not small enough, we must choose more frequency components given by (10) and repeat again the same iteration. Furthermore, the *compensational technique* [15] is used to improve the convergence ratio for the stiff circuits containing transistors and diodes.

4. Nonlinear Transmission Lines

Now, consider a nonlinear transmission line as shown in Fig. 3. The circuit equations are described by a pair of the following nonlinear partial differential equations:

$$-\frac{\partial v}{\partial x} = \frac{\partial \phi_L}{\partial t} + v_R, \quad -\frac{\partial i}{\partial x} = \frac{\partial q_C}{\partial t} + i_G \tag{23}$$

where

$$\phi_L = Li_L + \epsilon\hat{\phi}_L(i_L), \quad v_R = Ri_R + \epsilon\hat{v}_R(i_R) \tag{24.a}$$

$$q_C = Cv_C + \epsilon\hat{q}_C(v_C), \quad i_G = Gv_G + \epsilon\hat{i}_G(v_G) \tag{24.b}$$

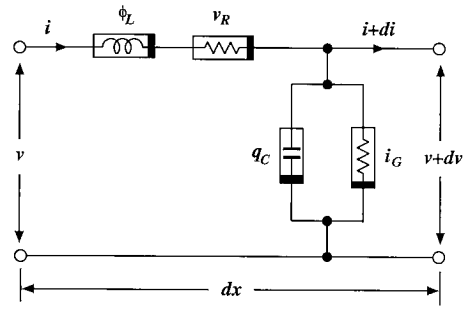

Fig. 3 Discrete model of nonlinear transmission line.

where $\hat{\phi}_L(i_L)$, $\hat{v}_R(i_R)$, $\hat{q}_C(v_C)$ and $\hat{i}_G(v_G)$ imply nonlinear terms, and ϵ means a small constant. We have $i = i_L = i_R$ and $v = v_C = v_G$ from Fig. 3. Substituting (24.a), (24.b) into (23), we have

$$-\frac{\partial v}{\partial x} = L\frac{\partial i}{\partial t} + Ri + \epsilon\left(\frac{\partial \hat{\phi}_L}{\partial i}\frac{\partial i}{\partial t} + \hat{v}_R\right) \tag{25.a}$$

$$-\frac{\partial i}{\partial x} = C\frac{\partial v}{\partial t} + Gv + \epsilon\left(\frac{\partial \hat{q}_C}{\partial v}\frac{\partial v}{\partial t} + \hat{i}_G\right). \tag{25.b}$$

When the nonlinear terms are small enough, we can efficiently apply the perturbation technique. Thus, we assume the waveforms at the $j+1$-st iteration:

$$v^{j+1}(x,t) = \sum_{k=-M}^{M} V_k^{j+1}(x)\exp(jk\omega t) \tag{26.a}$$

$$i^{j+1}(x,t) = \sum_{k=-M}^{M} I_k^{j+1}(x)\exp(jk\omega t) \tag{26.b}$$

Substituting (26.a), (26.b) into (25.a), (25.b), we have

$$\frac{d}{dx}\begin{bmatrix} V_k^{j+1}(x) \\ I_k^{j+1}(x) \end{bmatrix} = \begin{bmatrix} 0 & -Z_k \\ -Y_k & 0 \end{bmatrix}\begin{bmatrix} V_k^{j+1}(x) \\ I_k^{j+1}(x) \end{bmatrix} + \epsilon\begin{bmatrix} \hat{V}_k^j(x) \\ \hat{I}_k^j(x) \end{bmatrix} \tag{27}$$

where

$$Z_k = R + jk\omega L, \quad Y_k = G + jk\omega C.$$

The last term in (27) is estimated by

$$\left(\frac{\partial \hat{\phi}_L}{\partial i}\frac{\partial i}{\partial t} + \hat{v}_R\right)\Bigg|_{\substack{v=v^j \\ i=i^j}} \approx \sum_{k=-M}^{M} \hat{V}_k^j(x)\exp(jk\omega t) \tag{28.a}$$

$$\left(\frac{\partial \hat{q}_C}{\partial v}\frac{\partial v}{\partial t} + \hat{i}_G\right)\Bigg|_{\substack{v=v^j \\ i=i^j}} \approx \sum_{k=-M}^{M} \hat{I}_k^j(x)\exp(jk\omega t). \tag{28.b}$$

Thus, the nonlinear partial Eqs. (23) are transformed into a set of linear ordinary differential equations at each frequency component.

The solutions of (27) are given by

$$\begin{bmatrix} V_k^{j+1}(x) \\ I_k^{j+1}(x) \end{bmatrix} = \mathbf{\Phi}_k(x) \begin{bmatrix} V_k^{j+1}(0) \\ I_k^{j+1}(0) \end{bmatrix} - \epsilon \int_0^x \mathbf{\Phi}_k(x-s) \begin{bmatrix} \hat{V}_k^j(s) \\ \hat{I}_k^j(s) \end{bmatrix} ds \tag{29}$$

where $\mathbf{\Phi}_k(x)$ is the fundamental matrix solution of (27). In this case, it is given by

$$\mathbf{\Phi}_k(x) = \begin{bmatrix} \cosh \gamma_k x & -Z_{c,k} \sinh \gamma_k x \\ -\dfrac{1}{Z_{c,k}} \sinh \gamma_k x & \cosh \gamma_k x \end{bmatrix} \tag{30}$$

where

$$Z_{c,k} = \sqrt{\frac{R + jk\omega L}{G + jk\omega C}}$$

$$\gamma_k = \sqrt{(R + jk\omega L)(G + jk\omega C)}.$$

Since the numerical convolution integral is time-consuming, we introduce the recursive convolution technique based on the backward Euler method [18] at a point x_{i+1}.

$$\begin{aligned} \mathbf{z}(x_{i+1}) &= \int_0^{x_{i+1}} \mathbf{\Phi}_k(x_{i+1}-s) \begin{bmatrix} \hat{V}_k^j(s) \\ \hat{I}_k^j(s) \end{bmatrix} ds \\ &= \mathbf{\Phi}_k(\Delta x)\mathbf{z}(x_i) + \int_{x_i}^{x_{i+1}} \mathbf{\Phi}_k(x_{i+1}-s) \begin{bmatrix} \hat{V}_k^j(s) \\ \hat{I}_k^j(s) \end{bmatrix} ds \\ &= \mathbf{\Phi}_k(\Delta x)\mathbf{z}(x_i) + \Delta x \begin{bmatrix} \hat{V}_k^j(x_{i+1}) \\ \hat{I}_k^j(x_{i+1}) \end{bmatrix} \end{aligned} \tag{31}$$

where $\Delta x = x_{i+1} - x_i$.

Now, applying the Thevenin's theorem at the input terminal, we have

$$E_{in,k} - Z_{0,k} I_k^{j+1}(0) = V_k^{j+1}(0). \tag{32}$$

On the other hand, we have at the terminal point

$$V_k^{j+1}(l) = Z_{L,k} I_k^{j+1}(l) \tag{33}$$

Combining (29), (32) and (33), we can estimate the initial conditions $(V_k^{j+1}(0), I_k^{j+1}(0))^T$ at the input port, and $(V_k^{j+1}(x), I_k^{j+1}(x))^T$ are calculated by (29) and (31).

Now, we summarize our algorithm as follows:

1) Set $j = 0$. Put

$$(V_k^0(x), I_k^0(x))^T = \mathbf{0}, \quad (k = 0, 1, 2, \cdots, M)$$

as an initial guess. Set a sufficient small number δ for the stopping condition.

2) Set $j = j + 1$ and describe the nonlinear terms in Fourier expansions (28.a) and (28.b) by using FFT.

3) Calculate the zero state response given by the last term of (29).

4) Estimate initial guess from (29), (32) and (33).

5) Estimate the variation

$$\epsilon^{j+1} = \sum_{k=0}^{M} |V_k^{j+1}(0) - V_k^j(0)| + \sum_{k=0}^{M} |I_k^{j+1}(0) - I_k^j(0)|$$

and if $\epsilon^{j+1} < \delta$, then go to 6. Otherwise, go to 2.

6) Stop.

5. Illustrative Examples

5.1 Pulse Responses Analysis of Nonuniform Transmission Lines

To show the efficiency of our algorithm, consider a double line prototype chip interconnect shown in Fig. 4 (a)

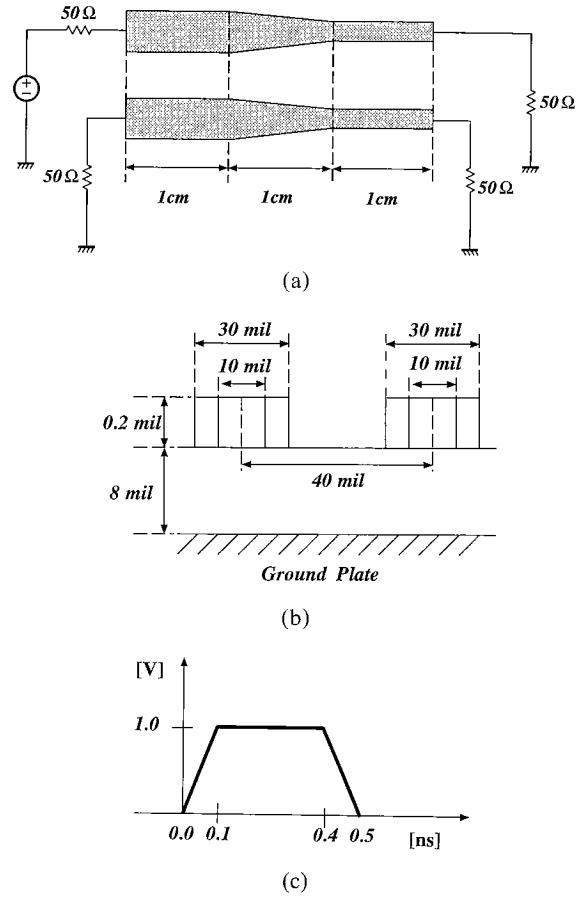

Fig. 4 (a) Nonuniform transmission lines. (b) Geometrical structure of the lines. (c) Input voltage source.

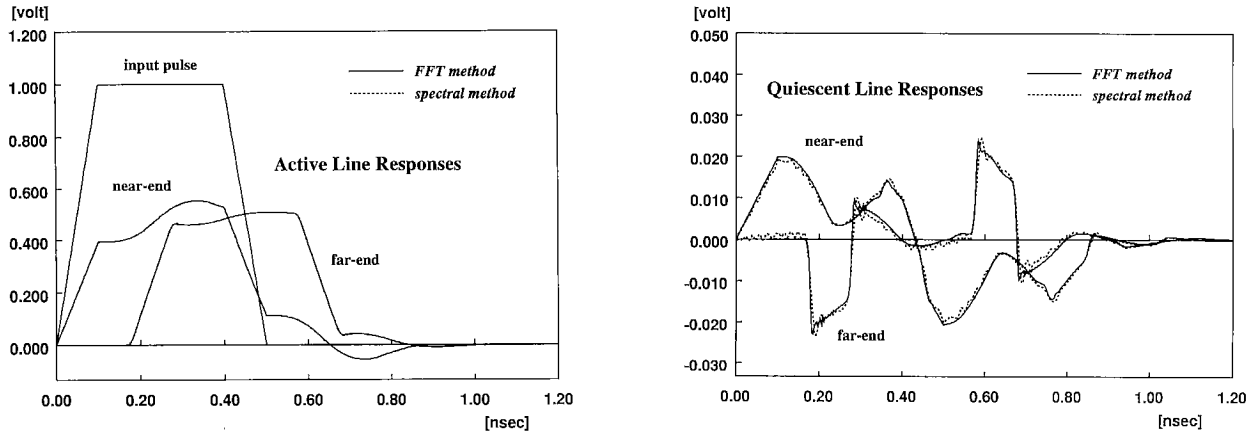

Fig. 5 (a) Transient responses at the active line. (b) Transient responses at the quiescent line.

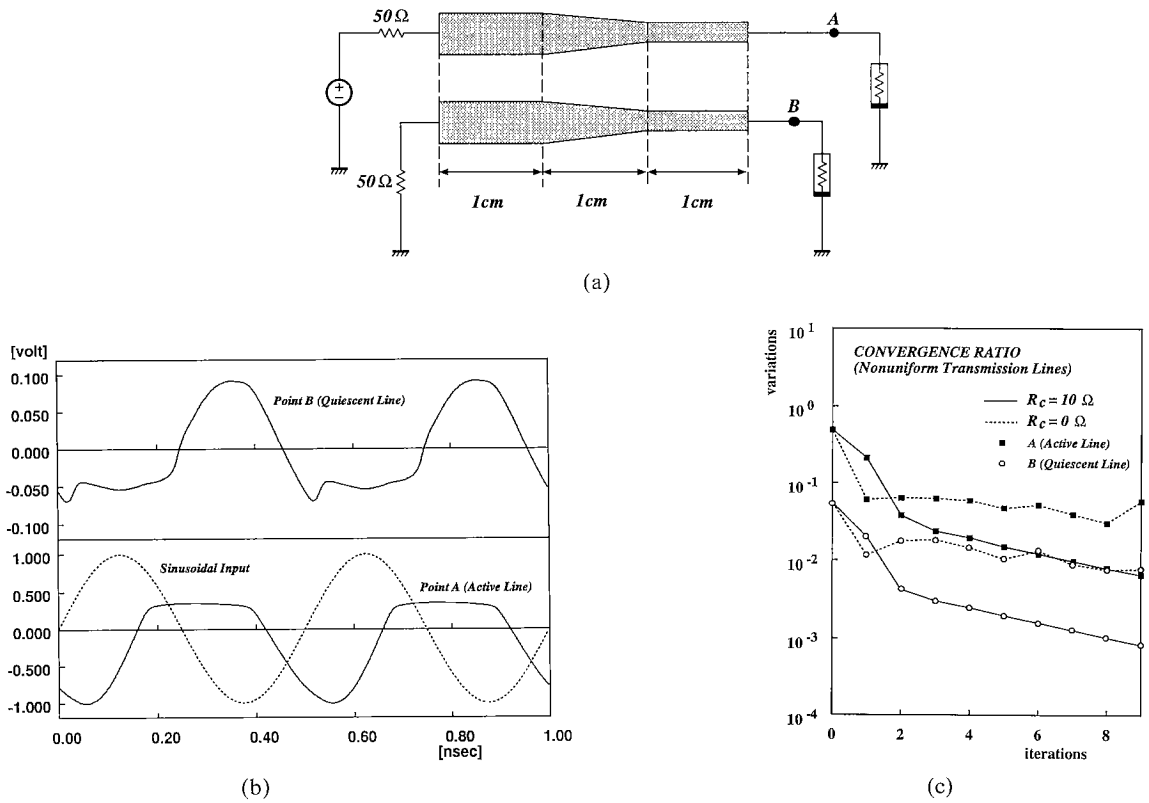

Fig. 6 (a) Nonuniform transmission lines with nonlinear termination. (b) Steady-state responses of nonuniform transmission lines at the partitioning point. (c) Convergence ratios.

and (b). The parameter matrices are as listed in table II of reference [6], and we assume that these matrices are piecewise linear in a distance x. The transient responses to the input voltage of Fig. 4(c) are computed using our method with 256 frequency components shown in Fig. 5(a) and (b). For the numerical integration, the step-sized is chosen by $\Delta x = l/300$. The results are compared with spectral method of Chebyshev interpolation [6], where 64 terms of Chebyshev polynomials and 1200 time points for numerical integration are taken into account. We get the same results in using more terms of Chebyshev polynomials, but inaccurate results of the quiescent lines to less time points. The proposed method is more accurate than spectral method, because

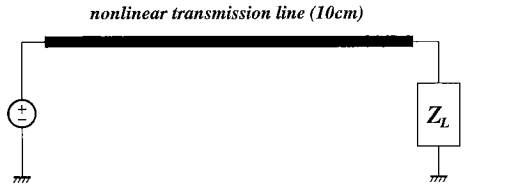

(a)

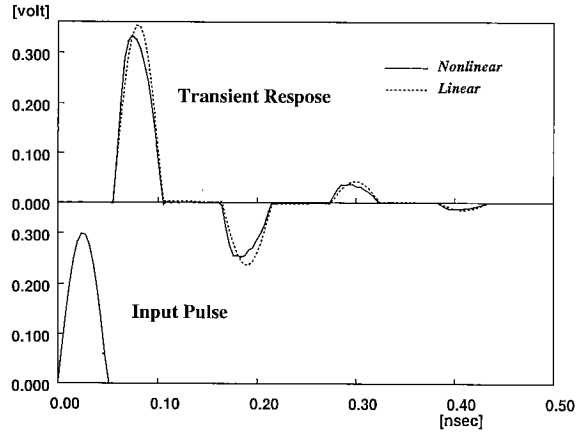

(b)

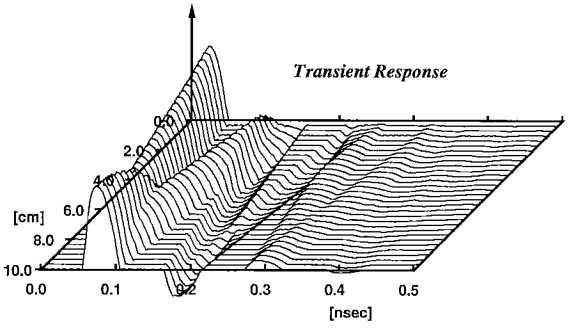

(c)

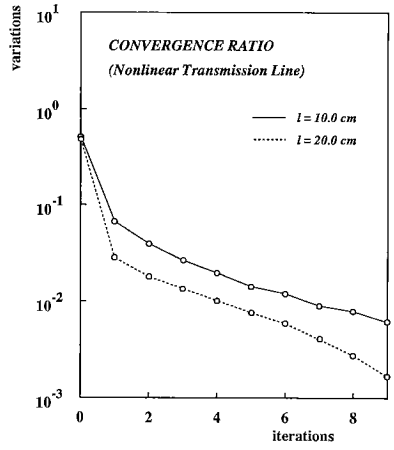

(d)

Fig. 7 (a) A nonlinear transmission line. (b) Transient Response at far-end. (c) Traveling Waveform. (d) Convergence ratios.

the quiescent lines do not respond until traveling waveform arrives at the far-end. The CPU time of the proposed method is 11.7 seconds and the CPU time of spectral method is 114.4 seconds on a Sun SPARC station 5. This shows that the proposed method is efficient.

5.2 Steady-State Analysis of Nonuniform Transmission Lines with Nonlinear Termination

Consider the same transmission lines in the previous example terminated by a nonlinear subnetwork as shown in Fig. 6 (a). The nonlinear resister is characterized by

$$I = 10\{\exp(40\,V) - 1\}\ [\mathrm{nA}].$$

We calculated the steady-state response to the input voltage source of a sinusoidal waveform as follows:

$$e(t) = 1.0\sin(\omega t)$$

where $2\pi/\omega = 0.5\,[\mathrm{ns}]$. The responses at the points A and B are shown in Fig. 6 (b) to 256 frequency components and $T = 1.0\,[\mathrm{ns}]$. In this example, our algorithm became unstable due to the strong nonlinearity. To improve the convergence, we introduced *compensation resistor* R_c [15] at each far-end of the lines. The efficiency is obvious in the convergence ratios as shown in Fig. 6 (c). The CPU time is 50.4 seconds on a Sun SPARC station 5.

5.3 Transient Analysis of Nonlinear Transmission Line

Consider a nonlinear transmission line terminated by a linear element shown in Fig. 7 (a). We assume that the nonlinear characteristics are given by

$$\hat{\phi}_L(i) = L_0(i - i^3/3), \quad \hat{q}_c(v) = C_0(v - v^3/3)$$
$$\hat{v}_R(i) = R_0(i + i^3), \quad \hat{i}_G(v) = G_0(v + v^3)$$

where

$$L_0 = 0.003\ [\mu\mathrm{H/cm}], \quad C_0 = 0.01\ [\mathrm{pF/cm}]$$
$$R_0 = 0.04\ [\mathrm{k\Omega/cm}], \quad G_0 = 0.04\ [\mathrm{mS/cm}]$$

and $Z_0 = 0$, $Z_L = 10\ [\mathrm{k\Omega}]$.

We calculated the transient response to the input pulse given by

$$e_{in} = \begin{cases} 0.3 \sin 10\omega t & (0 \leq t \leq \dfrac{T}{20} \text{ [ns]}) \\ 0 & (t > \dfrac{T}{20} \text{ [ns]}) \end{cases}$$

for $\omega T = 2\pi$. We consider 128 frequency components in our analysis. The dotted line in Fig. 7 (b) is the response of a linear transmission line neglecting the nonlinear terms. For the numerical integration, the step-sized is chosen by $\Delta x = l/120$. We can see that they give rise to large reflections from the source and terminal ports. Observe that the reflections at source port are reversed because the source impedance is zero, and those at terminal port are not reversed because of the terminal impedance 10 [kΩ]. On the other hand, the solid line shows the response of the nonlinear transmission line obtained by our perturbation technique. We found that the peaks of the waveforms are turned to the left. The phase velocity of the traveling wave [19] is given by

$$\frac{dx}{dt} = \pm \frac{1}{\sqrt{L(i)C(v)}} = \pm \frac{1}{\sqrt{L_0 C_0 (1 - i^2)(1 - v^2)}}$$

which means that the higher part of the wave is faster than the lower part of it. Thus, we can get the traveling waveform as shown in Fig. 7 (c). The convergence ratios for the different length of the transmission line are shown in Fig. 7 (d). The CPU time is 32.8 seconds on a Sun SPARC station 5.

6. Conclusions and Remarks

We have presented algorithms for calculating the steady-state responses of nonuniform transmission lines terminated by a nonlinear subnetworks and a frequency-domain perturbation technique for solving the nonlinear transmission line. Our method can be efficiently applied to weakly nonlinear transmission line. We need to improve the algorithm for analyzing the strong nonlinear transmission line.

Acknowledgment

The authors would like thank to Prof. Y. Shinohara and Dr. L. Jiang at Tokushima University for useful comments concerning with spectral method for transient analysis of nonuniform transmission lines.

References

[1] Y.C. Yang, J.A. Kong, and Q. Gu, "Time-domain perturbation analysis of nonuniform coupled transmission lines," IEEE Trans. Microwave Theory & Tech., vol.MTT-33, pp.1120–1130, Nov. 1985.

[2] F.Y. Chang, "Waveform relaxation analysis of nonuniform lossy transmission lines characterized with frequency-dependent parameters," IEEE Trans. Circuits & Systs., vol.38, pp.1484–1500, Dec. 1991.

[3] J.F. Mao and Z.F. Li, "Analysis of the time response of multiconductor transmission lines with frequency-dependent losses by the method of convolution-characteristics," IEEE Trans. Microwave Theory & Tech., vol.40, pp.637–644, April 1992.

[4] J.F. Mao and Z.F. Li, "Analysis of the time response of nonuniform multiconductor transmission lines with a method of equivalent cascaded network chain," IEEE Trans. Microwave Theory & Tech., vol.40, pp.948–954, May 1992.

[5] J.E. Schutt-Aine, "Transient analysis of nonuniform transmission lines," IEEE Trans. Circuits Systs.-I, vol.39, pp.378–385, May 1992.

[6] O.A. Palusinski and A. Lee, "Analysis of transients in nonuniform and uniform multiconductor transmission lines," IEEE Trans. Microwave Theory & Tech., vol.37, pp.127–138, Jan. 1989.

[7] T. Dhaene, L. Martens, and D.D. Zutter, "Transient simulation of arbitrary nonuniform interconnection structures characterized by scattering parameters," IEEE Trans. Circuits Systs.-I, vol.39, pp.928–937, Nov. 1992.

[8] S.L. Manney, M.S. Nakhla, and Q. Zhang, "Analysis of nonuniform frequency-dependent high-speed interconnects using numerical inversion of Laplace transform," IEEE Trans. Computer-Aided Design, vol.13, no.12, pp.1513–1525, Dec. 1994.

[9] T.J. Aprille, Jr. and T.N. Trick, "Steady-state analysis of nonlinear circuits with periodic input," Proc. IEEE, vol.60, pp.108–114, 1972.

[10] L.-T. Hwang and I. Turlik, "A review of the skin effect as applied to thin film interconnections," IEEE Trans. Components, Hybrids & Manuf. Technol., vol 15, no.1, pp.43–55, Feb. 1992.

[11] M.J.W. Rodwell, "Nonlinear transmission line for picosecond pulse compression and broadband phase modulation," Electron. Lett., vol.23, no.3, pp.109–110, 1987.

[12] C.J. Madden, R.A. Marsland, M.J.W. Rodwell, D.M. Bloom, and Y.C. Pao, "Hyperabrupt-doped GaAs nonlinear transmission line for picosecond shock-wave generation," Appl. Phys. Lett., vol.54, no.11, pp.1019–1021, 1989.

[13] R.H. Freeman and A.E. Karbowiak, "An investigation of nonlinear transmission lines and shock waves," J. Phys. D: Appl. Phys., vol.10, pp.633–643, 1977.

[14] Y. Tanji, Y. Nishio, and A. Ushida, "Analysis of nonuniform nonlinear transmission lines via frequency-domain method," Proc. JTC-CSCC'95, pp.635–638, July 1995.

[15] Y. Tanji, L. Jiang, and A. Ushida, "Analysis of pulse responses of multi-conductor transmission lines by a partitioning techniques." IEICE Trans. Fundamentals, vol.E77-A, pp.2017–2027, Dec. 1994.

[16] A. Ushida, T. Adachi, and L.O. Chua, "Steady-state analysis of nonlinear circuits based on hybrid methods," IEEE Trans. Circuits Systs.-I, vol.39, pp.649–661, Aug. 1992.

[17] L.O. Chua, "Introduction to Nonlinear Network Theory," McGraw-Hill, 1969.

[18] L.O. Chua and P-M. Lin, "Computer-Aided Analysis of Electrical Circuits: Algorithms and Computational Techniques," Prentice-Hall, Inc., 1975.

[19] D.T. Bickley, "Wave propagation in nonlinear transmission lines with simple losses," Electron. Lett., vol.2, pp.167–169, May 1966.

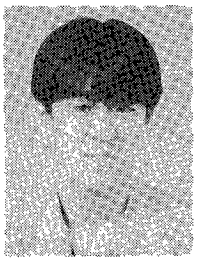

Yuichi Tanji was born in Shizuoka, Japan, on 1967. He received the B.E. and M.E. degrees from Tokushima University, Tokushima, Japan, in 1993, 1995, respectively. He is currently working towards the Ph.D. degree at the same university. His research interest is in circuit simulation.

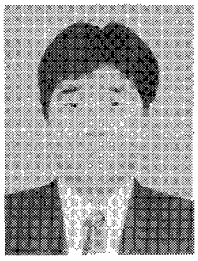

Yoshifumi Nishio received the B.E. and M.E. and Ph.D. degrees in Electrical Engineering from Keio University, Yokohama, Japan, in 1988, 1990 and 1993, respectively. In 1993, he joined the Department of Electrical and Electronic Engineering at Tokushima University, Tokushima, Japan, where he is currently an Assistant Professor. His research interests are in chaos and synchronization phenomena in nonlinear circuits. Dr. Nishio is a member of the IEEE.

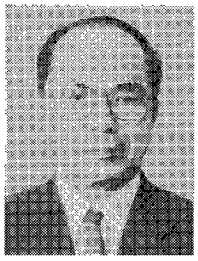

Akio Ushida received the B.E. and M.E. degrees in electrical engineering from Tokushima University in 1961 and 1966, respectively, and the Ph.D. degree in electrical engineering from University of Osaka Prefecture in 1974. He was an associate professor from 1973 to 1980 at Tokushima University. Since 1980 he has been a Professor in the Department of Electrical Engineering at the university. From 1974 to 1975 he spent one year as a visiting scholar at the Department of Electrical Engineering and Computer Sciences at the University of California, Berkeley. His current research interests include numerical methods and computer-aided analysis of nonlinear systems. Dr. Ushida is a member of the IEEE.